CLM - P 84

United Kingdom Atomic Energy Authority

RESEARCH GROUP

Preprint

THE CUSP COMPRESSION OF COLLIDING PLASMA BLOBS

T. K. ALLEN
K. DOBLE
T. J. L. JONES
R. M. PAYNE
I. J. SPALDING

Culham Laboratory,

Culham, Abingdon, Berkshire

1965

UNCLASSIFIED
(Approved for Publication)

CLM - P 84

THE CUSP COMPRESSION OF COLLIDING PLASMA BLOBS

by

T.K. ALLEN
K. DOBLE
T.J.L. JONES
R.M. PAYNE
I.J. SPALDING

Submitted for publication in Physics of Fluids

A B S T R A C T

A plasma formed by colliding two plasma blobs (in which the ions have a mean directed energy of 250 eV) is compressed by a rising cusp field which reaches 34 kG between the coils in 15 μsec. The plasma density and temperature rise to peak values of 10^{16}/cc and 7×10^5 °K, 5 - 6 μsec after the start of the compression. The escape hole at the ring cusp is found to be two ion gyro-radii wide and the hole size at the spindle cusps has a comparable total area. The containment time of 5-10 ion transits is consistent with that predicted using a simple 2-fluid model of effusion through a hole $2r_i$ wide at the ring cusp, with comparable losses through the spindle cusps. It is thought that field-shorting effects account for the observed hole size, but the possibility of anomalous diffusion has not been excluded. (This paper is a more detailed account of experiments previously described in an invited paper read before the American Physical Society at the New York Meeting, 4th November, 1964.)

U.K.A.E.A. Research Group,
Culham Laboratory,
Nr. Abingdon,
Berks.

September, 1965 (MEA)

CONTENTS

1. INTRODUCTION

One class of magnetic configuration which is of interest in thermonuclear fusion research is the open-ended trap containing field-free ($\beta = 1$) plasma. In units of the ion transit time across the trap, the density containment is measured roughly by the ratio of the total surface area of the plasma to the area of the loss holes at the constriction produced by the magnetic cusps. Typical examples of such traps are provided by the (long) high-β theta-pinch, which has neutral stability to the gross MHD instabilities, and "cusped" traps having positive MHD stability (of the type discussed by Berkowitz et al.[1]). Assuming that gross stability is achieved during the creation of hot plasma in such traps, the "reactor feasibility" of such systems hinges on

(a) the minimum hole size which can be established <u>in principle</u> at the cusps, i.e. whether a collision-free boundary layer can be broadened (by micro-instabilities) to widths comparable to the ion gyro radius.

(b) "technological" difficulties encountered wherever the field lines intersect the walls of the vacuum vessel. (These include possible short-circuiting of space-charge fields associated with any sheath thinner than the ion gyro radius, and energy losses by thermal conduction along the field lines.)

(c) impurity radiation losses - a problem common to all systems.

The present paper discusses the trapping, stability, and confinement of a high β plasma in cusped geometry. The purpose of the experiment is to measure the hole size of the trapped plasma and relate this to other measured plasma parameters (in particular, the energy containment time).

Some earlier work[2,3] (hereafter referred to as Papers I and II respectively) described the compression and containment of a shock-heated plasma by a spindle-cusped magnetic field which rose to 35 kG in 15 μsec. Under suitable conditions the plasma appeared to be grossly stable but the energy containment time was governed primarily by classical diffusion of plasma from a field-free central region into a thin boundary layer whose thickness was comparable to the resistive skin depth. (The latter was about three times larger than the ion gyro radius at the plasma boundary.) By suitably increasing the initial temperature of the plasma (i.e. its temperature <u>before</u> compression), it has proved possible to produce a plasma in which the skin depth calculated from the measured value of T_e (and postulating classical diffusion) is less than one half of the ion gyro radius. The plasma is now lost through a hole about two ion gyro radii wide at the ring cusp, so that the losses are primarily "cusp" losses of the type discussed by Berkowitz et al.[1].

The following experimental techniques have been used to examine the plasma:

(a) High speed framing photography (to examine the gross stability)

(b) Magnetic probes (to measure fields within the plasma for the first few μsec of the discharge only).

(c) He-Ne laser interferometry, absolute measurements of the optical continuum intensity, and observation of the plasma resonance in the far infra-red (to measure the electron density, n_e).

(d) Measurements of the absolute intensity of far infra-red bremsstrahlung, the relative intensity of Li-like impurity line radiation in the vacuum ultra-violet, and four-channel absorber measurements of soft X-ray emission (to determine the electron temperature, T_e).

(e) Retarding-potential analysis of the energy of ions escaping along the magnetic field lines beyond the ring cusp.

(f) A five-channel pressure probe analysis of the pressure distribution at the ring cusp and an ion probe scan of the losses at the spindle cusp (to measure the hole sizes directly).

2. APPARATUS AND OPERATION

The apparatus was geometrically identical to that described in Paper I and the cusp compression bank was also unaltered, but instead of colliding shock waves in a tube filled statically with hydrogen two plasma blobs now collide in a vacuum. The preheat system was modified to do this by introducing two fast-acting gas valves 6 cm behind the 10^{o} conical theta-pinch coils (Fig.1),i.e. the shock coils are now operated as conical theta-pinch guns. The valves were fired simultaneously 220 μsec before the application of a preionizing pulse of 20 kA (ringing at 1¼ Mc/s) to the coils. The main theta-pinch discharge was energised 3.5 μsec later, giving a peak current of 200 kA within 1.2 μsec. The discharge was short-circuited at the end of the first half-cycle, so that discrete blobs were ejected from the two opposing guns at a time $t \sim 0.8$ μsec after firing the theta-pinch. (The mean energy of the blobs is controllable by variation of the gas pressure - i.e. by variation of the valve to theta-pinch delay. A high pressure and low mean energy was chosen to improve the trapping efficiency in the rising cusp field, and also to produce the maximum number of particles).

The blobs were ejected with a mean translational energy of 250 eV (measured by time-of-flight at distances of 256 and 408 cms from the gun with the retarding potential analyser described in Section 3E); they carried a trapped field of ~ 70 gauss, and had an axial spread of velocities such that most of the blob arrived at the centre of the tube (i.e 20 cms

from the gun) within 3 μsec. The blobs partially randomised upon collision (at time $t = 1.9$ μsec) in a manner outlined previously[4]. The neutral hydrogen pressure (measured with a fast ionization gauge by firing the fast valves only) was of the order 1–2 mTorr in the cusp region at the time of arrival of the blobs, and the base pressure of the apparatus was 10^{-6} Torr. The time of arrival of the blobs at the centre of the tube was confirmed with a 3.39μ helium-neon laser interferometer[5], and the density averaged over the radial direction was greater than 2×10^{15}/cc. The cusp confining field (which rises sinusoidally to 35 kG in 15 μsec) was normally energised at a time $\tau = 1.5$ μsec after the gun – i.e. just as the blobs were passing through the cusp coils, and slightly before their collision. Density-sensitive signals, such as the optical and infra-red continuum intensities, were rather less sensitive to this cusp delay than were the temperature-sensitive (soft X-ray, grazing incidence and pressure probe) signals. The delay of 1.5 μsec was thus an empirical compromise between firing too early (when little plasma was able to enter the trap) and firing too late (i.e. after the plasma had cooled by contact with the walls).

3. THE COMPRESSION MEASUREMENTS

A. Framing Camera Pictures

The compression of the colliding plasma was photographed (in a 10" o.d. cylindrical vacuum vessel) using an STL image converter camera with exposure times of 10 and 20 nsec. Fig.2a shows three successive stages during one compression (at intervals of 500 nsec). The plasma appears to be grossly stable; the three vertical bars are of instrumental origin. The radius of the optical boundary (at 45^{o} to the z axis) is plotted in Fig.12d; photography at later stages of the compression was hindered by intense emission of light at the ring cusp due to particle bombardment at the walls. At abnormally long delays between firing the guns and the cusp bank it was noticed that the plasma showed evidence of flute instabilities (Fig.2b). This observation strengthens by contrast the conclusion that the plasma shown in Fig.2a is stable, and the fluted structure also permits one to look for rotation of the surface. Using a 20 nsec exposure, no rotation was observed with 50, 100, 200, or 500 nsec intervals between three successive frames. (It is probable that a surface velocity greater than 10^{7} cm/sec could have been detected.)

B. Magnetic Probe Measurements

A single 3.3 mm diameter magnetic probe sheathed in a 5 mm o.d. quartz tube was used to measure B_p, the radial magnetic field on the median plane within the plasma. Fig.3 shows the instantaneous ratio of B_p to the vacuum field B_v as a function of time, at

the position ($r = 1.75$ cm, $z = 0$). The cusp field is excluded for 2-3 μsec and then appears to reach the vacuum value some 4 μsec after firing the cusp. Some small, systematic, fluctuations of field during the first few μsec were associated with the preheat system, but careful adjustment of the time at which the thetatron was short circuited reduced the mean level of these fluctuations to zero for the first 2-3 μsec of the compression. (The amplitude of the fluctuations was then ± 50 gauss at a distance of 1.75 cm from the axis.) The presence of the probe certainly enhances the rate at which field penetrates into the plasma, as framing photographs show axial assymetries after a few μsec when the probe is immersed in the plasma. Moreover, the continuum emission in the infra-red is doubled by the insertion of the probe, and impurity radiation near 4010 Å is increased by a factor of about 100. We conclude that $\beta = 1$ for at least 3 μsec, but that no conclusions can be drawn after this time (i.e. once the quartz sheath has been heated by plasma bombardment)[6,7].

C. Infra-red and Optical Continuum Measurements

Measurements were made of the intensity of bremsstrahlung emission in the far infra-red between the wavelengths 60 -700μ, with a spectral resolution of 7% and a time response of ½ μsec. The experimental arrangement was similar to that described in Paper II; two photoconductive detectors cooled in liquid helium were used - an indium antimonide detector covered the range 100-700μ, and In-Ge the range 60-100μ. The discharge was viewed at an angle of 10^{o} to the median plane; the acceptance cone of the copper light pipe and grating spectrometer was such that there was a sharp cut-off in sensitivity outside a cone having a diameter of 5 cm at the centre of the discharge. Higher order diffraction spectra were removed by a suitable combination of scattering gratings and a glass transmission filter.

Fig.4a shows the emission at 150μ from two colliding blobs and Fig.4b that of three overlays at 225μ with a compression field of 27 kG. Two overlays of detector noise are also shown in the latter picture to indicate typical signal/noise ratios for the experiment. Oscillograms similar to Fig.4b were taken at fourteen wavelengths between 70 and 600μ and the emission as a function of wavelengths was plotted for various times during the discharge (vide Paper II). Fig.5 is a typical plot obtained at one instant of the discharge; it shows clearly the sudden drop in emission which occurs at frequencies less than the electron plasma frequency, which is equivalent to a maximum density of 10^{16}/cc at this time. The density deduced from the cut-off is shown for other stages of the compression in Fig.12a; n_e reaches a maximum 6 μsec after firing the cusp and falls by 20% in the next 6 μsec. The point of inflexion which occurs in Fig.4b about 4 μsec after the cusp has fired is also noticed (to a much smaller extent) on pictures taken at even shorter wavelengths; high speed photography

indicates that at this time during the compression the plasma no longer completely fills the acceptance cone of the infra red spectrometer, and the plasma diameter is therefore about 5 cm at this time.

Simultaneous measurements were also made of the absolute intensity of the optical continuum at 4010 Å (Fig.4c), and the derived values of n_e are shown in Fig.12a. The density agrees well with that determined from the infra-red measurements. It should be noted that in the optical measurements the intensity was averaged along a line-of-sight which was 50 cm long, and one therefore viewed not only confined plasma, but also lower density plasma which had already escaped along the field lines at the ring cusp. The density containment time should therefore be an over estimate.

D. Electron Temperature Measurements

Soft X-ray Emission

Soft X-rays were emitted by the plasma and their energy spectrum was determined by measuring the attenuation through aluminium foils. Aluminised NE 102 phosphors were used with EMI 9524 S photomultipliers to detect the emission from a cone having a diameter of 3 cm at the centre of the discharge. A typical (single channel) absorption plot is compared in Fig.6 with the theoretical absorption curve computed for bremsstrahlung emission from a pure, thermal, hydrogen plasma at temperatures of kT_e = 100 eV and 60 eV. The plot suggests some excess of very soft photons (e.g. line radiation) but the slope is broadly consistent with kT_e = 70 eV. The computed curve for kT_e = 100 eV is taken from Jahoda et al.[8], and their data was extrapolated to obtain the curve for kT_e = 60 eV. The X-ray signals were sensitive to the thetatron-cusp delay (τ), their intensity increased by a factor 3 when the compression field was increased from 34 to 41 kG, and they were completely quenched when a 10% argon in hydrogen mixture was used in the place of pure hydrogen. Moreover, when both guns were fired the X-ray intensity was 3-4 times that produced by one gun and it is therefore thought that the signals are indeed volume (bremsstrahlung) X-rays, rather than X-rays produced at the walls of the vessel.

A 4-channel absorption spectrometer was also used to give single-shot temperature measurements and a typical set of signals (where were extremely smooth and reproducible) is shown in Fig.7. (The gain of the 3.6 mg/cm^2 channel is approximately × 200 that of the 1.5 mg/cm^2 channel). Transverse magnetic fields of ~ 1 kG and suitable collimators reduced the possibility of foil bombardment by energetic electrons. The spectra obtained with this multi-channel instrument were similar to, but slightly softer than, the averaged data given

in Fig.6. (For this particular experiment the fields at the spindle and ring cusps had been reduced by some 15% by the fracture, and subsequent removal, of the field - shaping inserts shown in Fig.1.)

Impurity Line-ratio Measurements

The ratio of the intensity of the $2s^2S_{1/2} - 2p^2P^o_{3/2}$ transition to the (unresolved) $2s^2S_{1/2} - 3p^2P^o_{1/2,3/2}$ transitions has been measured for the Li-like impurity ions NV, OVI and NeVIII. When $n_e < 10^{16}$/cc, the determination of these ratios should give a good measure of T_e[9], provided a relative calibration of the spectrometer is available at the relevant wavelengths, which lie in the vacuum ultraviolet. A 1 metre grazing incidence monochromator was used for the experiments, with the grating set at 5^o for NV and OVI, and 2^o for NeVIII; a closed photomultiplier coated with sodium salicylate was used as the detector. A relative calibration between 150 Å and 1240 Å was obtained by using Zeta as a spectroscopic (standard) source under conditions identical to those used originally by Heroux[9]. (A more direct calibration was also available at the particular wavelengths 237 Å and 1085 Å, by measuring the branching ratio between $n = 5$ to $n = 1$ and $n = 2$ transitions in HeII[10].) It has not yet been possible to extend the calibration down to 88 Å, but the 88 Å NeVIII line was sufficiently strong to strengthen conclusions drawn from the NV and OVI measurements.

Typical OVI (1031.9 Å and 150.1 Å) and NeVIII (770.4 Å and 88.1 Å) signals are shown in Fig.8a. Each line was scanned for a few Å on either side of the peak, and the long wavelength doublets were resolved and identified. No N_2 or O_2 were added to the discharge but the Ne measurements were made with a 1% Ne in H_2 mixture. (The CIV 1548 Å line was only observed for a few shots after first pumping the system and then all carbon lines disappeared as the discharge cleaned up.) To illustrate the overall reproducibility of the discharge, several traces are shown at each wavelength. Fig.8b shows the effect of reducing the valve-thetatron delay, and 8c of increasing τ. The OVI ratio (at peak signal) is given in Table I for various delays and values of compression field and the ratio is found to vary in a sensible way with these parameters. The time variation of T_e is shown in Fig.12b. The electron temperature was derived from the measured line ratios in the manner discussed by Heroux (i.e. using Seatons' collisional excitation cross-sections averaged over a Maxwellian distribution of electron velocities).

TABLE I

Temperature Scaling Experiments

	OVI 1031.9/150.1 Å (Uncorrected) Line Ratio	kT_e (eV)	Time of peak signal t (μsec)
(a) θ - Cusp Delay (B_c = 27 kG)			
τ = 1.5 μsec	1.43(14)	45	5
τ = 3.5 μsec	4.22(63)	24	3.5
(b) Compression Field			
B_c = 27 kG	1.43(14)	45	5
B_c = 38 kG	1.02(25)	65	3.8
(c) Valve to Preionizer Delay (B_c = 27 kG)			
τ = 200 μsec	1.37(21)	47	4.8
τ = 220 μsec	1.43(14)	45	5.0
τ = 240 μsec	1.11(16)	60	4.0

To measure the NeVIII 88 Å/770 Å intensity ratio it was necessary to use the maximum available compression field (42 kG); the experimental ratio (uncorrected for the relative transmission of the spectrometer at the two wavelengths) was then 4.4 ± 2.8 at peak signal (~ 5.5 μsec after firing the cusp). A reliable calibration of the spectrometer is not yet available at the wavelengths 88 Å/770 Å; however, typical gratings are more sensitive at 200 Å than 1000 Å by factors of 3-30, and so unless there is an order of magnitude increase in sensitivity between 200 and 88 Å we conclude that T_e should exceed 7×10^5 °K.

It should be noted that when $n_e = 10^{16}$/cc and $T_e = 7 \times 10^5$ °K, the electron-electron relaxation time $\tau_{ee} = 6 \times 10^{-10}$ sec, and so the electron velocity distribution should be Maxwellian. Moreover, the reciprocal transition probability for the levels involved is ~ 10^{-8} sec, which is also small compared to the plasma time scale of 10^{-6} sec, so that the line ratio should give a good measure of the electron temperature provided that

(a) the theoretical excitation cross-sections employed are correct[9]

(b) there are no strong gradients of electron temperature in the discharge

(c) the electron velocity distribution is indeed Maxwellian

These measurements have shown that T_e is high (i.e. 50-100 eV) at the time of maximum density, that it increases with increase of the compression field, and that it does not vary rapidly over the first 2-8 μsec of the discharge (i.e. over the time for which the OVI lines are sufficiently intense for accurate measurement.)

E. Ion Energy Measurements

A retarding-potential ion energy analyser[11] was used (in the absence of any guide field) at distances of 256 cm and 408 cm from the theta-pinch gun to measure the ion energies in a blob ejected from a single gun. The mean energy was 250 eV - a value which agreed with time-of-flight measurements down the drift tube. The analyser was then placed radially with its axis in the plane of symmetry between the two opposing guns (i.e. parallel to the field lines at the ring cusp) and its 0.005 inch diameter pinhole at $r = 44$ cms, $z = 0$, where the field was 660G at the time when the field between the coils was 38 kG. The radial field variation was such that in the absence of collisions the ion motion should be adiabatic out to the detector; the drift tube was sufficiently large to admit ions with $W_1 = 1$ keV. A typical signal is shown in Fig.9, where it may be compared to one taken without the cusp field. The early part of the signal had a mean energy in excess of 200 eV and a definite time of origin corresponding to the time of ejection of the blobs from the guns; this signal represents fast, untrapped plasma which is channelled out by the rising cusp field. At later times the mean ion energy is less than 200 eV and there is no definite time of origin; this 'time smudging' is characteristics of containment within the cusp bottle. A typical set of energy histograms is shown in Fig. 10. Theoretical analysis of the flow of plasma from a boundary region into a confining field which converges towards the cusp coils (so forming a magnetic mirror which varies with time from 1:1 to 4:1 at the ring cusp), and then into the diverging field beyond, is complicated by the fact that the ion-ion mean free path and the ion gyro radius are both comparable to the channel dimension.

Despite the consequent difficulties in quantative analysis of the data it is qualitatively apparent from Fig. 10 that energetic ions are confined by the cusp field for times of the order 10 μsec. Whether one employs a collisionless or collision-dominated model of plasma flow along the field lines, the mean energy $W_{\parallel}$ measured at the detector should lie between $\frac{3}{2} kT_i$ and $\frac{5}{2} kT_i$; thus if one takes $W_{\parallel} \sim 80$ eV, T_i is roughly $4\text{–}6 \times 10^5\ ^{o}K$. It should be noted that the plasma density is sufficiently high in the cusp experiment for space-charge effects at the detector to be possible; however, qualitative confidence in this method is derived from the fact that the signals were sensibly controlled by the grid potentials. (A measurement of the proton temperature is required in order to determine the ion gyro radius; we have used the retarding-potential method merely to confirm the value inferred by taking $T_i = T_e$, where T_e is known spectroscopically to reach $7 \times 10^5\ ^{o}K$.)

F. Determination of Hole Size

The spatial distribution of the pressure exerted by plasma escaping at the ring cusp was measured with an array of four pressure probes. These probes were 2 mm diameter acoustic-line piezo-electric gauges having response times of less than 1 μsec, and described in detail in Paper II. The probes were spaced linearly 4 mm apart, were parallel to the median plane (Fig.1) and themselves defined a plane at 30^{o} to the median plane; thus their projected spacing across the ring cusp was 2 mm.

The probes were first placed at a position ($r = 15$ cm, $z = 0$) just beyond the field maximum at the ring cusp; all the probes detected an initial short transient pulse produced by escaping (untrapped) plasma, but long-lived pressure signals were observed thereafter on only one or two of the probes. This suggested that the hole size was comparable to the diameter of the probes at the ring cusp, and the probes were therefore withdrawn into the diverging field region (at $r = 20$ cm, $z = 0$), where the half-to-half intensity pressure width (Δ) was larger than the 2 mm resolution of the probes. A typical pressure profile obtained during a single discharge is shown by the ringed points in Fig.11(a) and (b); further points were obtained from subsequent discharges. It should be noted that the hole size is considerably less at 2.4 μsec after firing the cusp than at the earlier time of 1.4 μsec. A typical pressure signal is reproduced in Fig.9(a) and the variation of Δ with time is plotted in Fig.11(c) for two values of valve to theta-pinch delay. Δ is slightly larger for the shorter delay - i.e. for the delay corresponding to a higher energy per particle in the injected blobs.

A single, cranked, 5 mm O.D. biassed Faraday Cup (having a pinhole of 0.005 inch diameter) was subsequently inserted near one of the guns in order to estimate the size of the loss hole at the spindle-cusp. The probe was situated at the point of maximum field at the spindle cusp (i.e. at $r = 0$, $z = 10$ cm) and the peak field at this position was 26 kG (while the corresponding field at the ring cusp was 35 kG.) After it had been established that the presence of this ion probe made no significant difference to the pressure signals measured at the ring cusp, the probe was racked across the cusp; four measurements of the ion current in the z direction were made at each radial position of the probe, and an (averaged) plot of the ion current distribution at the spindle cusp was thus obtained. The full half-width of the distribution decreased almost linearly from 3.6 cm at 1 μsec after firing the cusp, to 1.2 cm at 7 μsec. (A similar ion probe was then used to measure the hole size at the ring cusp, $r = 12$ cm, $z = 0$. The cusp width fell from 3 mm at 1 μsec to $\sim$ 1 mm at 7 μsec. This result, which was averaged over many discharges, is broadly consistent with the pressure probe measurements discussed in the next section.)

4. DISCUSSION

A. Summary of the Plasma Parameters

Two plasma blobs, each containing about 2×10^{18} particles[12] and having a mean directed energy of 250 eV, collide and partially randomise between the cusp coils, which are energised at the instant of collision ($t = 0$). The plasma density rises from an initial value of 2×10^{15}/cc to a peak of 10^{16}/cc at $t = 5.5$ μsec (i.e. well before the peak magnetic field). About 50% of the particles are trapped by the rising cusp field. The initial value of T_i is approximately 10^6 °K and the initial value of T_e is estimated to be an order of magnitude lower; the relaxation times τ_{ii} and τ_{ee} are therefore of the order $\frac{1}{3}$ μsec and 10^{-10} μsec respectively and it is reasonable to assume that both the ions and electrons thermalize. The equipartition time (τ_{eq}) between the hot ions and cold electrons is also short, so that T_e rises rapidly to the measured value of 7×10^5 °K at $t = 4$ μsec. The resistive skin depth due to classical diffusion at this temperature is of the order 1 mm after 1 μsec which is the ion transit time out of the cusp; this should therefore be the <u>limiting</u> thickness of any boundary layer dominated by diffusion from field-free plasma into a layer from which plasma is subsequently lost along the field lines[3,13,14]. The ion temperature of this proton-electron plasma is difficult to measure directly; lower limits to T_i are therefore inferred from the spectroscopic measurements of T_e, and some qualitative support for this procedure is provided by the electrostatic analysis of ion energies at the ring cusp.

The ion gyro-radius at the plasma boundary is typically a few mm (i.e. 2-3 resistive skin depths) and it is therefore of interest to compare the measured cusp widths with the mean gyro radius $\overline{r_i}$. Let us take

$$\overline{r_i} = \sqrt{\frac{2\,kT_i}{M_i}} \cdot \frac{M_i\,c}{e\,B_c},$$

i.e. let the ion have a transverse energy kT_i in the maximum field B_c at the ring cusp. Some 4–5 μsec after the start of compression those particles which happen to escape from the field-free central region encounter a magnetic mirror of about 3:1 between the equilibrium surface and the field maximum B_c. Some plasma then escapes into the diverging field beyond the cusp, and in a collision-dominated situation the flow becomes supersonic as the temperature falls during the subsequent expansion. In the opposite limit of collision-free flow, and with the magnetic moment $\frac{W_\perp}{B}$ an adiabatic invariant, the gyro-radius should scale as $B^{-\frac{1}{2}}$. The present situation lies between these two extremes, since λ_{ii} = 2-20 mm, but it is

convenient nevertheless to use the $B^{-\frac{1}{2}}$ scaling law to estimate the variation of cusp width with r at the ring cusp. In particular, the detailed pressure measurements shown in Fig.11 were made at (r = 20 cm, z = 0) where the field is ¼ of the field maximum (at r = 11 cm, z = 0) and has diverged in the z direction by a factor of 2.2; it is therefore estimated that the cusp width measured between the coils (Δ_c) is one half of that measured at the pressure probes. This factor is quite consistent with ion probe and pressure probe measurements made directly at the line cusp. (The measurement at r = 20 cm is preferred because it is a multi-channel measurement.)

At t = 4 μsec the cusp width measured at the pressure probes is 3.2 mm (Fig.11c), hence Δ_c = 1.6 mm; this is to be compared with the ion gyro radius $\overline{r_i} \geqslant 0.75$ mm (since $T_i \geqslant T_e = 7 \times 10^5\ ^oK$). The electron temperature is known less accurately at other times during the compression, but Sections 3D and E indicate that T_i does not vary rapidly for the first 6-7 μsec thus at t = 1.4 μsec $\overline{r_i}$ = 2.1 mm, compared to Δ_c = 2.8 mm. The pressure probe measurements therefore indicate that the plasma escapes through a well defined circumferential 'hole' centred on the median plane, that this becomes narrower as the compression field rises, and that the hole size at the ring cusp is roughly $\overline{2r_i}$. Similar conclusions are drawn from the ion probe measurements at the spindle cusp, but here the hole is a circle of radius 6-10 $\overline{r_i}$ so that the losses through the spindle cusps are some 60% of that through the line cusp. (The diameter of the spindle cusp hole is expected to be larger than the width of the hole at the ring cusp because of the field divergence at the plasma boundary, cf. Grad[16].)

B. Comparison of Theoretical and Experimental Containment Times

The adiabatic compression of a high β hydrogen plasma in a spindle-cusp geometry has been computed numerically using a simple 2-fluid hydrodynamic model[15]. The model used involves two modifications to that discussed in Paper II:[3,14]

(a) Separate energy equations are written for the ions and electrons, namely

$$3/2\ \frac{d}{dt}\ (NkT_i) = -\ (nkT_i)\ \frac{dV}{dt} + 5/2\ (kT_i)\ \frac{dN}{dt} + 3/2\ \frac{Nk(T_e - T_i)}{\tau_{eq}} \qquad \ldots\ (1)$$

and

$$3/2\ \frac{d}{dt}\ (NkT_e) = -\ (nkT_e)\ \frac{dV}{dt} + 5/2\ (kT_e)\ \frac{dN}{dt} - 3/2\ \frac{Nk(T_e - T_i)}{\tau_{eq}} \qquad \ldots\ (2)$$

where

$$\tau_{eq} = \frac{3\ M_i}{8\sqrt{2\pi}\ e^4 m_e^{\frac{1}{2}}\ \log\ \Lambda}\ \ \frac{(kT_e)3/2}{n}\ \ \text{(Spitzer)}$$

and N is the number of ions or electrons in the contained volume $V = \frac{32\pi}{105} R_p^3$.

(b) It is postulated that plasma is lost primarily by a process of effusion through a hole two ion gyro radii wide at the ring cusp. Diffusion losses are ignored, so that the loss rate through the ring cusp is given by

$$\frac{dN}{dt} = \frac{\overline{n v_i}}{4} \cdot \frac{M_i v_i}{e B_c} \cdot 2\pi R_p$$
$$= -\frac{3\pi n k T_i}{2} \cdot R_p \cdot \frac{C}{e B_c} \qquad \ldots (3)$$

where R_p is the mean plasma radius, v_i is the ion velocity, and the bar denotes an average over a Maxwellian velocity distribution. The computed variation of n_e, T_e, T_i and R_p is compared in Fig.12(a-d) with experiment. Note that

(i) The initial values of $T_i = 10^6\ ^oK$ and $T_e = 6 \times 10^4\ ^oK$ have been estimated for this calculation - the value of T_i is consistent with the experiments of Section 3E and the initial value of T_e does not affect the calculation strongly.

(ii) The curves a and b correspond to 0 and 50% losses through the spindle cusps relative to a ring cusp hole of area $(2\pi R_p \cdot 2\pi \overline{r_i})$.

(iii) Energy losses by radiation and by thermal conduction along the field lines have been neglected in the energy balance. It may be shown[14] that the energy loss by plasma flow should predominate over the loss by thermal conduction when

$$\frac{\lambda_{ee}}{R_p} < \left(\frac{M_e}{M_i}\right)^{1/2}.$$

Now the ratio of electron-electron mean free path to plasma dimension is 0.03 when $T_e \sim 7 \times 10^5\ ^oK$ and 0.008 when $T_e = 3.5 \times 10^5\ ^oK$, so that thermal conduction losses should not dominate in the present experiment. (It may be noted that both n_e and T_e peak 5-6 μsec after the beginning of the compression, whereas T_e should peak earlier than n_e if the energy losses were radiation or conduction dominated.) It is concluded that within the limitation of the model used, there is adequate agreement between the experimental and theoretical containment times.

C. Plasma Hole Size and Stability

At temperatures sufficiently high that collisional diffusion is unimportant, the cusp hole size is expected to be intermediate in size between the electron and ion gyro radii[16,17]. The measured hole is found to be two ion gyro radii wide at the ring cusp (within an estimated accuracy rather better than a factor of 2). Possible explanations for this observation are:

(1) β is less than 1 at the instant of initial confinement. (The magnetic probe observations of Section 3B discount this possibility.)

(2) There is anomalous diffusion driven by universal or two-stream instabilities.

(3) The space-charge field between ions and electrons at the plasma boundary may be short-circuited by low-conductivity plasma produced where the field lines intersect the glass wall of the vessel[18].

There is no conclusive evidence to discount (2), although it is noteworthy that both the ion signals and soft X-ray signals are very smooth. (Both the detectors have frequency responses of $\sim$ 10 Mc/s, i.e. approaching the ion cyclotron frequency.) However, the possibility of electron plasma oscillations can be definitely excluded since the absolute intensity of the infra-red emission near the plasma frequency is rather less than that calculated for thermal emission from a quiescent plasma of density 10^{16}/cc and temperature $\sim 10^{6}\ ^{o}$K. (This situation may be contrasted with that discussed by Adamov et al.[19] for some z and theta-pinches in which runaway electrons are believed to have excited plasma oscillations. Such non-equilibrium plasmas have been shown to emit radiation near the electron plasma frequency with an intensity several orders of magnitude greater than the thermal radiation power. In these experiments the X-ray and microwave emission also varied in an irregular way during the discharge.) The probability is high, therefore, that the third mechanism is of major importance, as no precautions have been taken to avoid short-circuiting effects in this experiment.

5. CONCLUSIONS

A high β plasma has been established in a spindle-cusped magnetic field. The escape hole between the coils at the ring cusp is two ion-gyro radii wide, and the hole size at the spindle cusps is comparable in total area to that at the ring cusp. Framing camera pictures show the plasma to be grossly stable during compression and the intensity of the soft X-ray and infra-red emission are both consistent with radiation from a thermal plasma. The containment time (roughly five to ten ion transits) is consistent with that predicted using a simple 2-fluid hydrodynamic model of effusion through a hole $\overline{2r_i}$ wide at the ring cusp (with a comparable loss through the spindle cusps). It is thought that field shorting effects account for the observed hole size, but the possibility of anomalous diffusion has not been excluded.

6. ACKNOWLEDGEMENTS

The authors wish to acknowledge the help of Mr. J.N. Burcham in preliminary experiments, the continuing assistance of Messrs A.J. Hawkes and A.F. Newman, the engineering support given by Mr. T.E. James and his team and the co-operation of Mr. B. Powell during the grazing incidence calibration on ZETA. The infra-red measurements were made in collaboration with Mr. M.F. Kimmett of RRE Malven. Finally, we thank Drs. R.J. Bickerton and R.S. Pease for their interest in this work.

7. REFERENCES

1. BERKOWITZ, J. et al. Second Int. Conf. on Peaceful Uses of Atomic Energy, Geneva Proceedings, 31, 171 (1958).

2. ALLEN, T.K., McWHIRTER, R.W.P., and SPALDING, I.J. Nuclear Fusion 1962 Supplement Pt.1, 67 (1962)

3. ALLEN, T.K. and SPALDING, I.J. (to be published in Physics of Fluids, November 1965.)

4. ALLEN, T.K., and COX, A.J. Bull Amer. Phys. Soc., series 2, 8, 424 (1963).

5. ASHBY, D.E.T.F., and JEPHCOTT, D.F. Appl. Phys. Letters 3, 13 (1963)

6. KEILHACKER, M. Nuclear Fusion 4, 287 (1964).

7. JAHODA, F.C. and SAWYER, G.A. Phys. Fluids 6, 1195 (1963)

8. JAHODA, F.C., et al. Phys. Rev. 119, 843 (1960)

9. HEROUX, L. Proc. Phys. Soc. 83, 121 (1964). It should be noted that Seatons' cross-sections have recently been questioned by Burke P.G. and Tait J.H. (Unpublished).

10. GRIFFIN, W.G., and McWHIRTER, R.W.P. Proceedings of the Conference on Optical Instruments and Techniques, Ed. K.J. Habell (London: Chapman Hall) p.14 (1962)

11. MASON, D., J. Nucl. Energy Pt. C 6, 553 (1964).

12. CRUDDACE, R.G. Culham Laboratory. Unpublished information 1965.

13. WRIGHT, J.K., and PHILLIPS, N.J. J. Nucl. Energy Pt. C 1, 240 (1960).

14. BICKERTON, R.J. Culham Laboratory. Unpublished information. 1964.

15. HOBBS, G., and SPALDING, I.J. Culham Laboratory. Unpublished information.

16. GRAD, H. Progress in Nuclear Energy Series XI, Plasma Physics, Vol.II, 189 (1963)

17. ROSENBLUTH, M.N. Dynamics of a pinched gas. In: Landshoff, R.K.M. ed. Magneto hydrodynamics: a symposium, Stanford University press, 1957.

18. TAYLOR, J.B. J. Nucl. Energy Pt. C 4, 401 (1962) ASHBY, D.E.F.T., and AVIS, B.E. Bull Am. Phys. Soc. Series 2, 9, 331 (1964)

19. ADAMOV, I. et al. J. Nucl. Energy Pt. C, 7, 83 (1965).

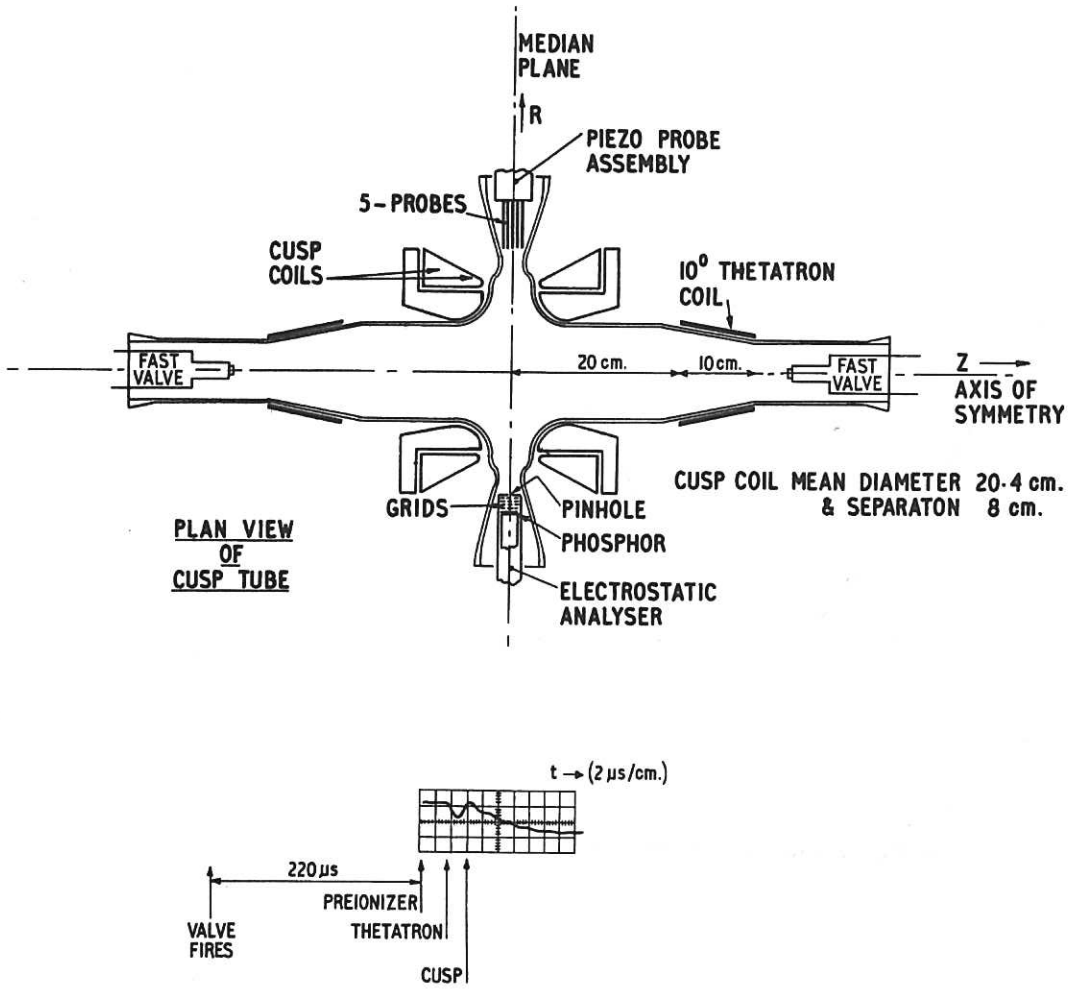

Fig. 1 (CLM-P84)
Schematic diagram of the apparatus and firing sequence

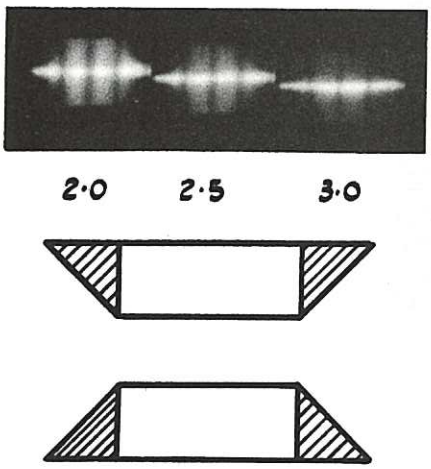

Fig.2(a) (CLM-P84)
Stable compression at times t = 2.0 μsec, 2.5 μsec and 3.0 μsec during a single shot (10 nsec exposure)

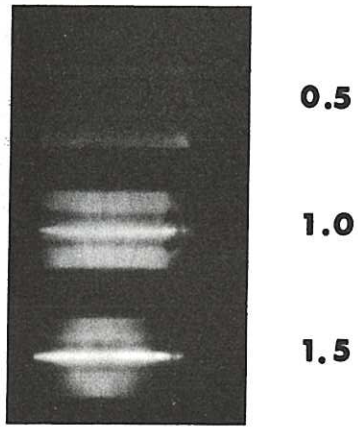

Fig.2(b) (CLM-P84)
Unstable compression (of dirty plasma) at t=0.5, 1.0, 1.5 μsec (10 nsec exposure)

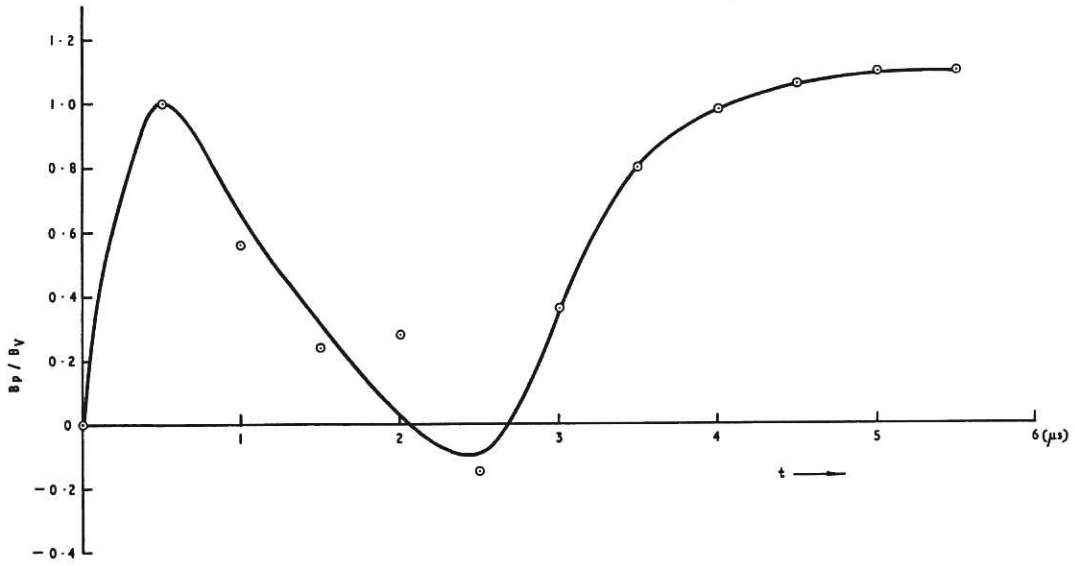

Fig. 3 (CLM-P84)

B_p/B_V as a function of time at r = 1.75 cm, z = 0

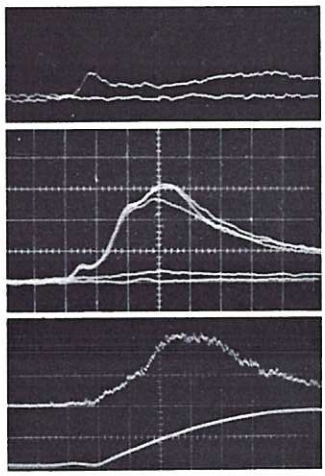

Fig. 4 (CLM-P84)

(a) Infra red emission at 150 μ from colliding blobs. (All horizontal scales 2 μsec/cm): (b) Infra red emission at 225 μ from cusp (B_C= 27 kG). The trace shows three overlays of the emission superimposed on two overlays of detector noise: (c) Upper trace - Optical continuum at 4010 Bottom trace - Cusp waveform

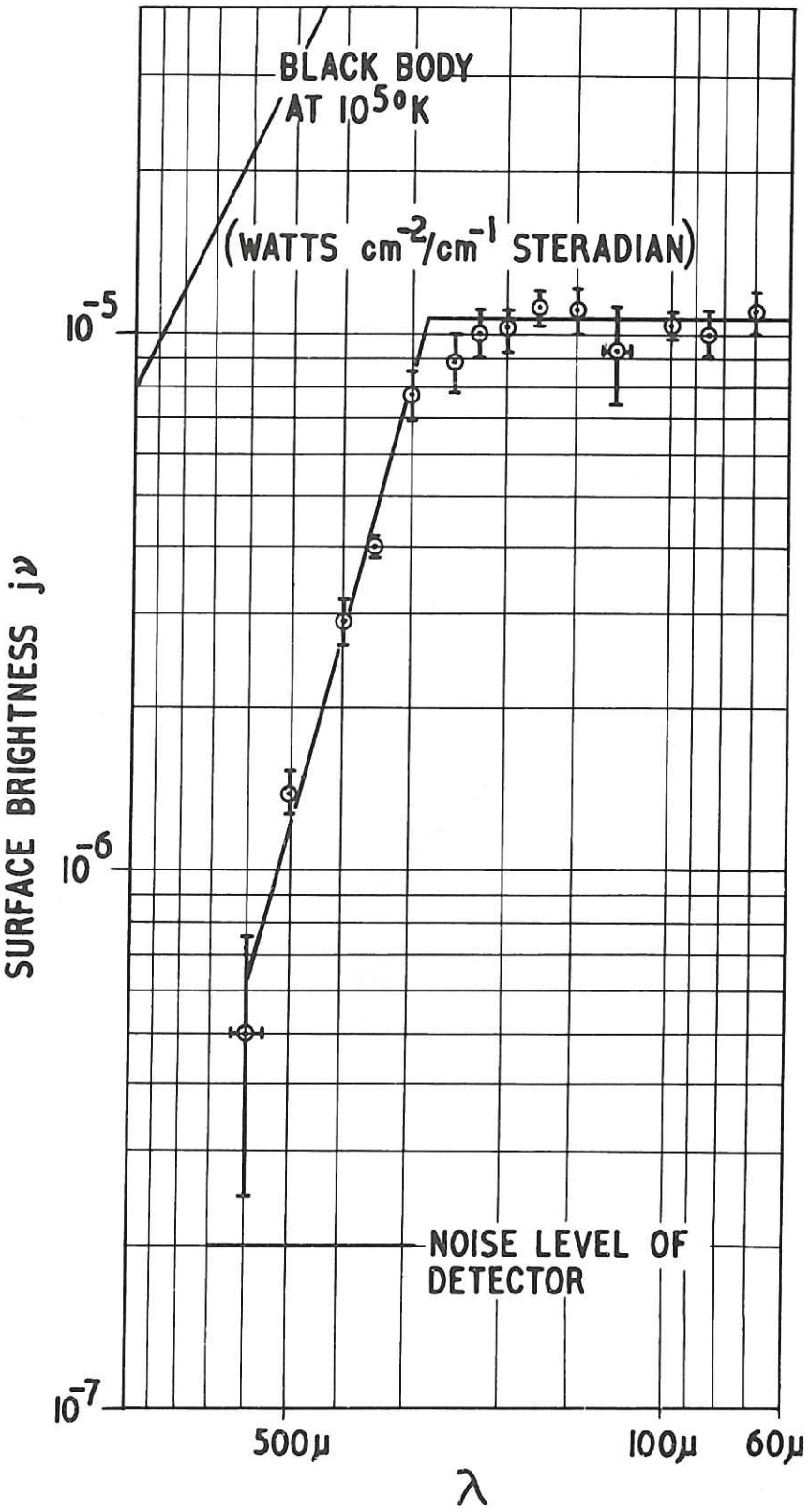

Fig. 5 (CLM-P84)
Plot of infra red emission at t = 4 μsec (B_c = 27 kG)

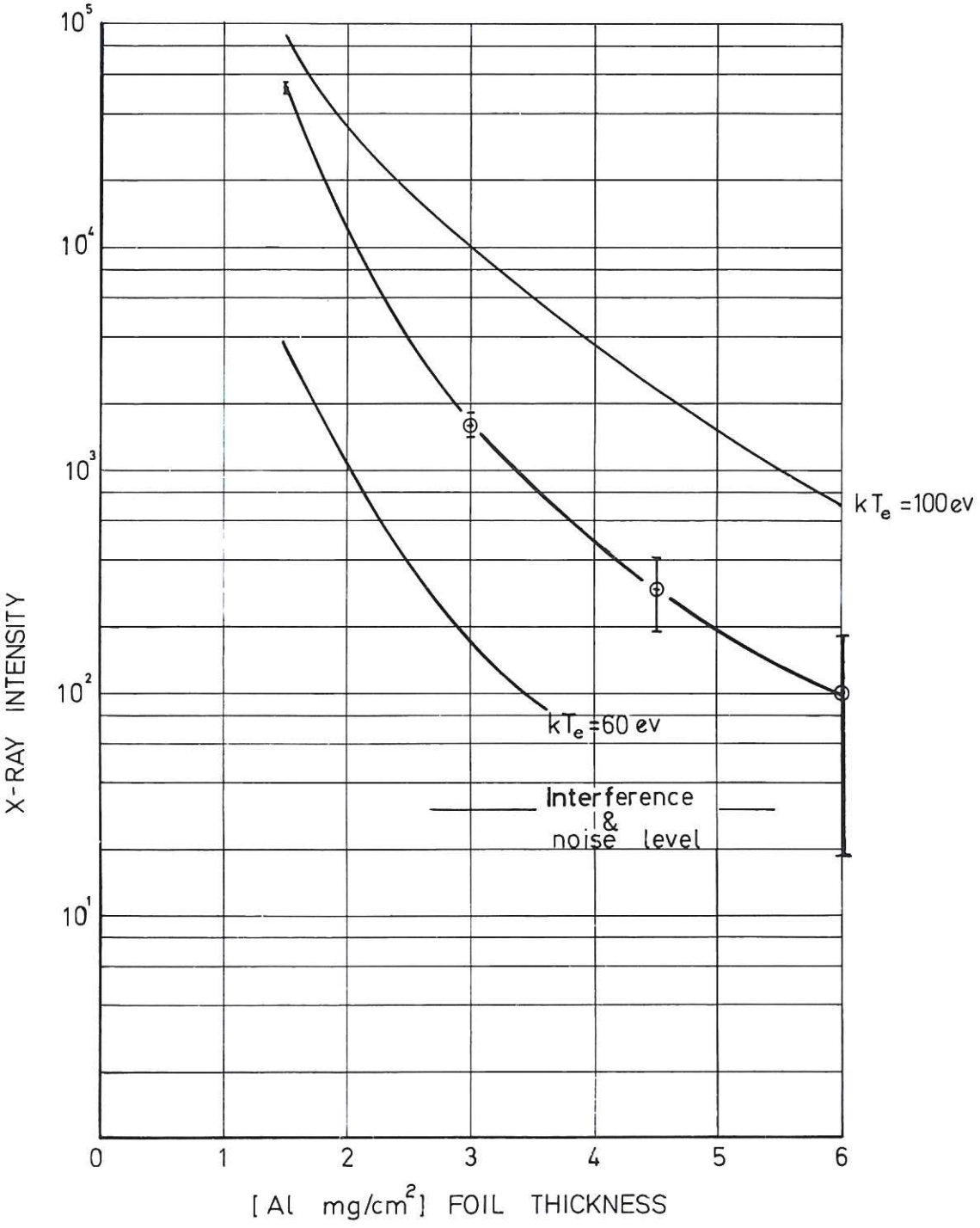

Fig. 6 (CLM-P84)
Absorber plot of x-ray emission at t = 4 μsec (B_c = 34 kG)

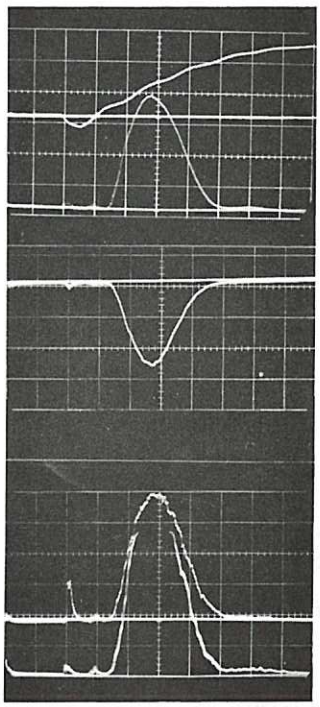

TI – 22·9·64

Fig. 7 (CLM-P 84)

4 channel x-ray signals (B_c = 34 kG). (Horizontal scale 2 μsec/cm; top trace cusp field - triggered by preionizer)

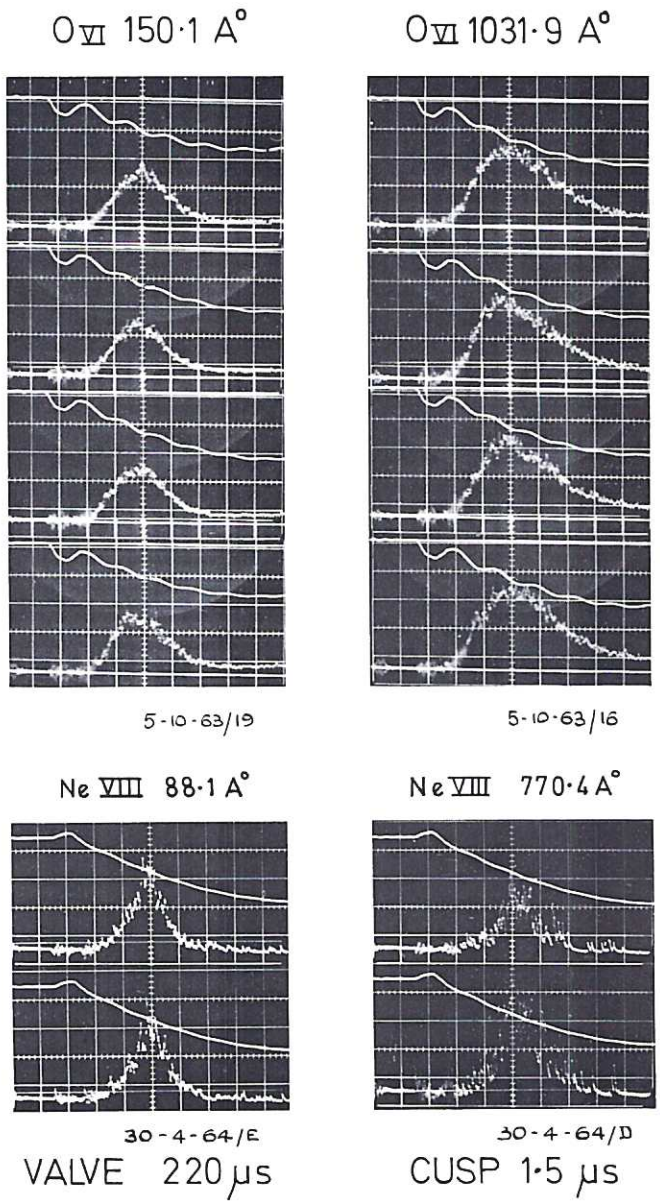

Fig. 8(a) (CLM-P84)
OVI line radiation (B_c = 27 kG) and NeVIII lines (B_c = 43 kG)

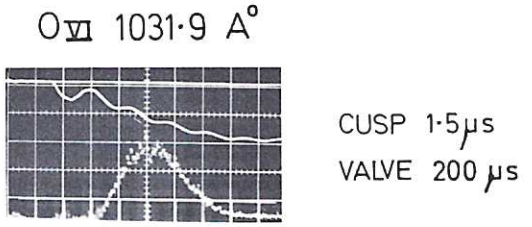

Fig. 8(b) (CLM-P84)
The effect on the OVI 1031.9 Å line of shortening the valve delay

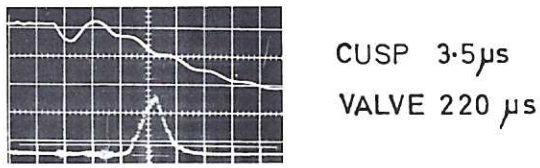

Fig. 8(c) (CLM-P84)
The effect on the OVI 1031.9Å line of increasing the cusp delay

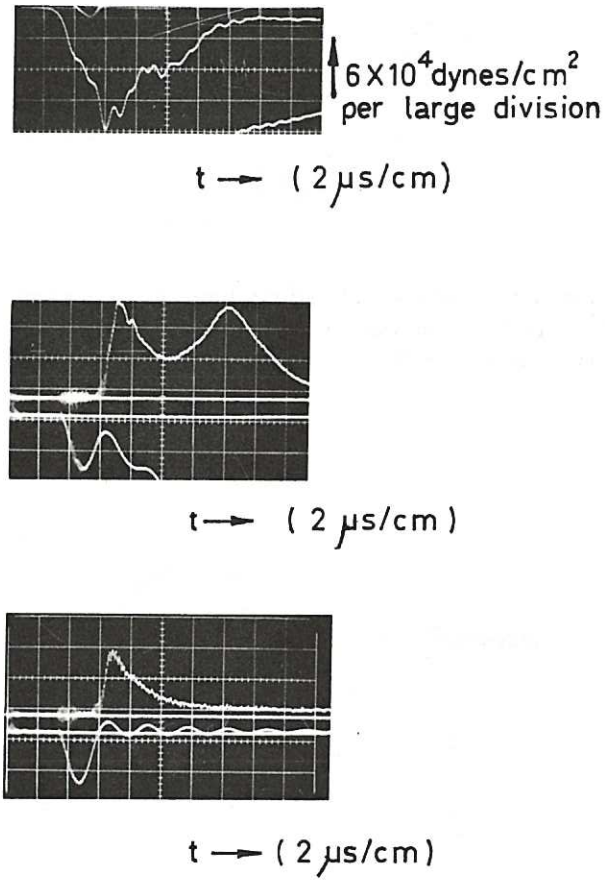

Fig.9 (CLM-P 84)

(a) Typical Piezo probe signal (B_C = 38 kG): (b) total ion current with cusp field B_C = 27 kG: (c) total ion current from colliding blobs. (Gain increased)

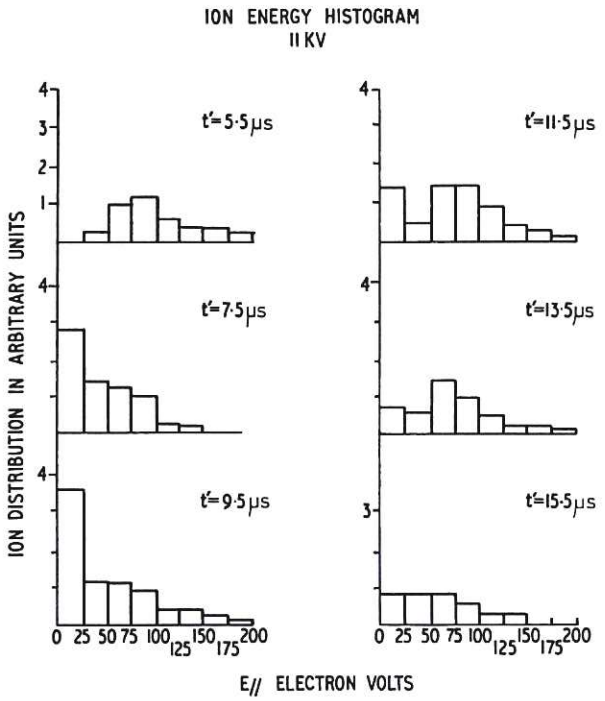

Fig. 10 (CLM-P84)

Ion energy histograms at various times (t′) after firing the cusp. (B_c = 38 kG) (Note that an ion transit time correction of 3 - 4 μsec should be substracted from t′ to relate the measurements to events occurring at the centre of the discharge.)

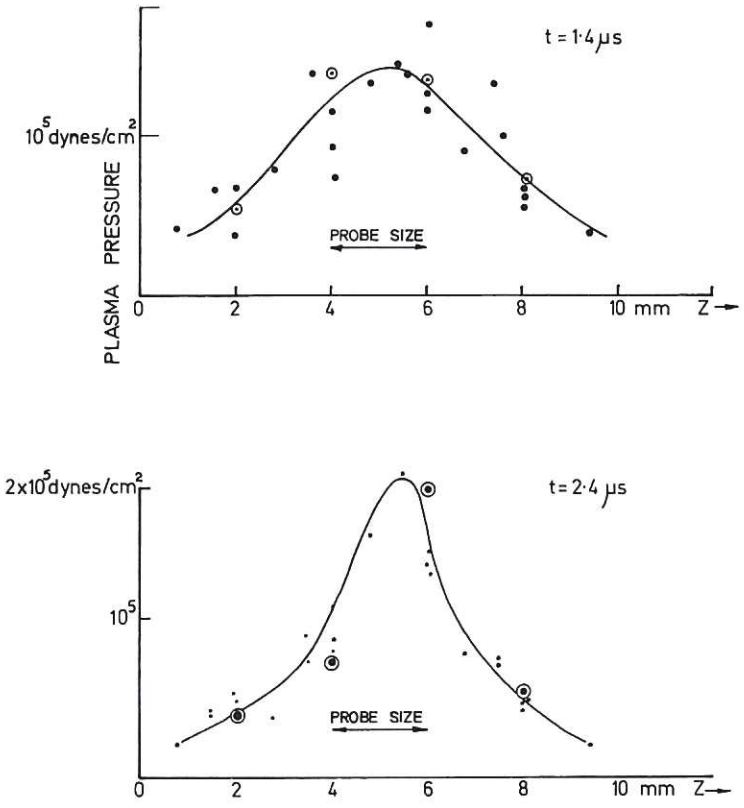

Fig. 11(a)
and 11(b) (CLM-P84)

Pressure profiles at time t = 1.4 and 2.4 μsec for B_c = 38 kG. (Gun delay 200 μsec.) Position r = 20 cm, z = 0

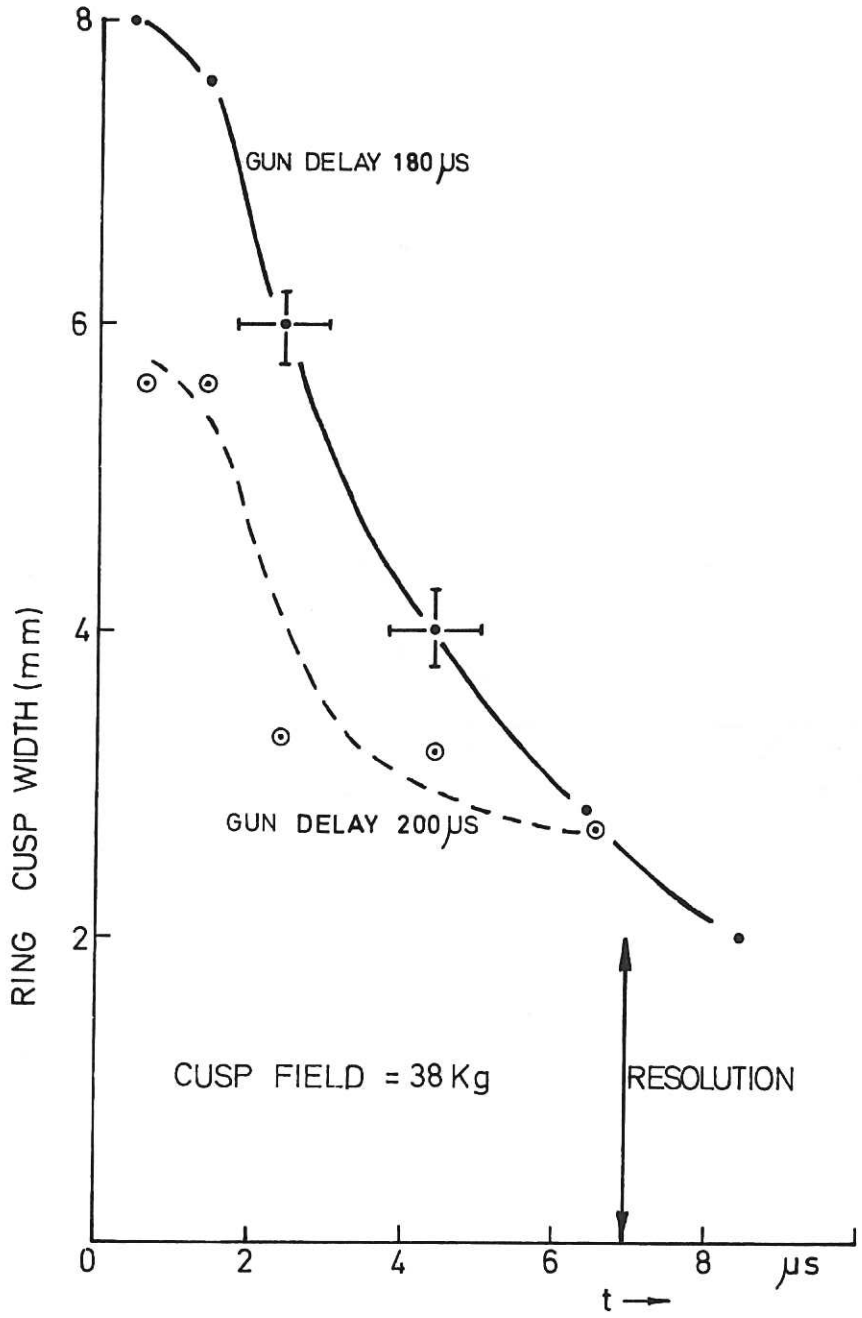

Fig. 11(c) (CLM-P84)
Time resolved cusp width for gun delays of 180 and 200 μsec (at r = 20 cm, z = 0)

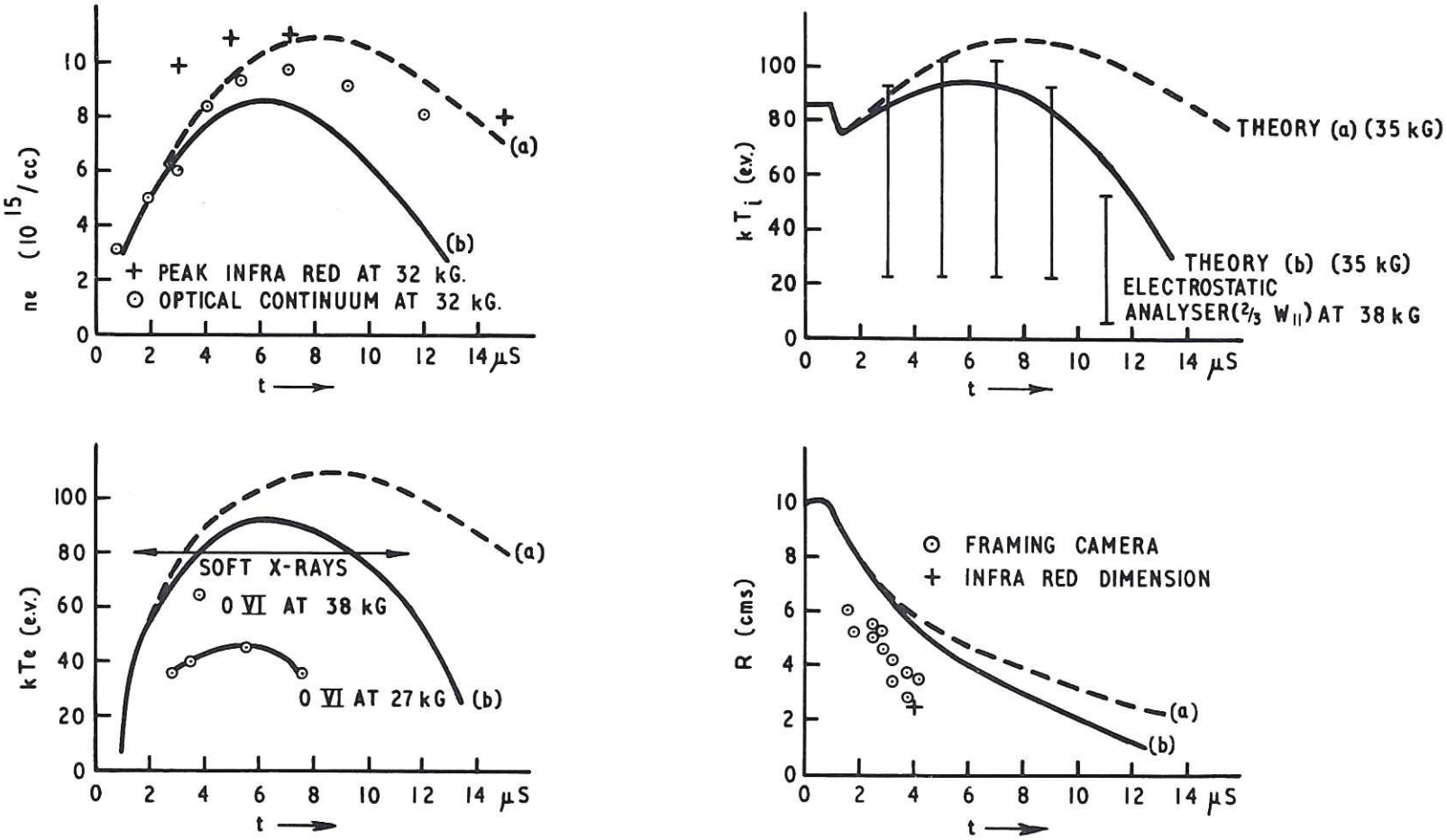

Fig. 12 (CLM-P84)

Time variation of n_e, T_e, T_i, and the plasma radius R_p compared with numerical calculations. (The framing camera data was measured at 45^0 to the z axis.)

Computed curve (a) for loss through ring cusp ($\Delta = 2r_i$) only. ($B_c = 35$ kG.)

(b) 50% additional loss through point cusps. ($B_c = 35$ kG.)